Earth's Future

RESEARCH ARTICLE
10.1029/2019EF001189

Key Points:
- Twenty-two percent of populated and agricultural areas of the Northern Hemisphere concurrently experienced hot extremes between May and July 2018
- It is *virtually certain* that these 2018 northhemispheric concurrent heat events could not have occurred without human-induced climate change
- We would experience a GCWH18-like event nearly 2 out of 3 years at +1.5 °C and every year at +2 °C global warming

Supporting Information:
- Supporting Information S1

Correspondence to:
M. M. Vogel and S. I. Seneviratne,
martha.vogel@env.ethz.ch;
sonia.seneviratne@ethz.ch

Citation:
Vogel, M. M., Zscheischler, J., Wartenburger, R., Dee, D., & Seneviratne, S. I. (2019). Concurrent 2018 hot extremes across Northern Hemisphere due to human-induced climate change. *Earth's Future*, *7*, 692–703. https://doi.org/10.1029/2019EF001189

Received 20 FEB 2019
Accepted 23 MAY 2019
Accepted article online 7 JUN 2019
Published online 3 JUL 2019

©2019. The Authors.
This is an open access article under the terms of the Creative Commons Attribution-NonCommercial-NoDerivs License, which permits use and distribution in any medium, provided the original work is properly cited, the use is non-commercial and no modifications or adaptations are made.

Concurrent 2018 Hot Extremes Across Northern Hemisphere Due to Human-Induced Climate Change

M. M. Vogel[1], J. Zscheischler[1,2,3], R. Wartenburger[1], D. Dee[4], and S. I. Seneviratne[1]

[1]Institute for Atmospheric and Climate Science, ETH Zurich, Zurich, Switzerland, [2]Climate and Environmental Physics, University of Bern, Bern, Switzerland, [3]Oeschger Centre for Climate Change Research, University of Bern, Bern, Switzerland, [4]European Centre for Medium-Range Weather Forecasts, Reading, UK

Abstract Extremely high temperatures pose an immediate threat to humans and ecosystems. In recent years, many regions on land and in the ocean experienced heat waves with devastating impacts that would have been highly unlikely without human-induced climate change. Impacts are particularly severe when heat waves occur in regions with high exposure of people or crops. The recent 2018 spring-to-summer season was characterized by several major heat and dry extremes. On daily average between May and July 2018 about 22% of the populated and agricultural areas north of 30° latitude experienced *concurrent* hot temperature extremes. Events of this type were unprecedented prior to 2010, while similar conditions were experienced in the 2010 and 2012 boreal summers. Earth System Model simulations of present-day climate, that is, at around +1 °C global warming, also display an increase of concurrent heat extremes. Based on Earth System Model simulations, we show that it is *virtually certain* (using Intergovernmental Panel on Climate Change calibrated uncertainty language) that the 2018 north hemispheric concurrent heat events would not have occurred without human-induced climate change. Our results further reveal that the average high-exposure area projected to experience concurrent warm and hot spells in the Northern Hemisphere increases by about 16% per additional +1 °C of global warming. A strong reduction in fossil fuel emissions is paramount to reduce the risks of unprecedented global-scale heat wave impacts.

1. Introduction

Record-breaking temperatures occurred concurrently in multiple regions including North America, Europe, and Asia in late spring/summer 2018 (NOAA, 2018a, 2018b, 2018c). Europe experienced late spring and summer temperatures that were more than 1 °C warmer than 1981–2010 (Copernicus, 2019). The contiguous United States had the warmest May since 1895 (NOAA, 2018c), and the hottest month ever observed was in July in the Death Valley (NOAA, 2018a). The 2018 hot temperatures are in line with an increase in intensity and frequency of extreme heat events over many regions on land and in the ocean in recent years (Coumou & Rahmstorf, 2012; Christidis et al., 2014; Fischer & Knutti, 2015; Frölicher et al., 2018; Rowe & Derry, 2012; Seneviratne et al., 2014). Owing to their devastating impacts, understanding changes in extreme temperature events is highly relevant for society and ecosystems. Recent heat waves with particularly severe impacts include the 2010 Russian and 2015 Indian heat waves. The 2010 Russian heat wave was associated with the death of tens of thousands of people, major crop failure, millions of hectares affected by fires, and around 15 billion U.S. dollar economic loss (Barriopedro et al., 2011). During the 2015 heat wave in India, at least 2,500 people died (Ratnam et al., 2016). Impacts were particularly severe because they occurred in agricultural regions and/or regions with high population density.

Given the tremendous impacts of these heat waves, the question arises how much they can be attributed to human activities. Most recent heat waves have been attributed to a smaller or larger extent to anthropogenic climate change (NAS, 2016). For instance, anthropogenic climate change has tripled the occurrence rate of heat waves similar to the 2010 heat wave in Russia (Otto et al., 2012; Rahmstorf & Coumou, 2011). Heat waves of the magnitude of the Indian heat wave in May/June 2015 are 2 to 8 times more likely due to human-induced climate change (Wehner et al., 2016). A near-real-time attribution study concluded that the extreme heat in northern Europe in the 2018 summer was on average 2 times more likely due to human-induced climate change (World Weather Attribution, 2018). However, in these cases, as in many other heat wave attribution studies, natural variability cannot be excluded as a driver.

In the future, the intensity, frequency, and global heat wave area over land are projected to drastically increase (Coumou & Robinson, 2013; Christidis et al., 2014). These projected increases can strongly affect future heat wave impacts and risk of concurrent extremes. While locally confined climate extremes often lead to devastating impacts at the local scale, spatially correlated extremes can have much more severe societal impacts due to their effect on integrated variables. For instance, concurrent heat waves in different agricultural regions can affect global food production (Sarhadi et al., 2018) and consequently increase global food prizes and food insecurity (Tigchelaar et al., 2018). Similarly, synchronized river floods can cause excessive damages (Berghuijs et al., 2019).

In the present study, we investigate the exceptional nature of the 2018 north hemispheric heat wave in the context of anthropogenic climate change. We first synthesize reported heat-related impacts across the entire Northern Hemisphere in the spring to summer season. Subsequently, we investigate the fraction of the land area in the northern midlatitudes that is either densely populated or used for agricultural production and that was affected by extremely hot conditions. We then study whether current Earth System Models simulate a 2018-like area fraction under present-day conditions and whether the event could have occurred without climate change. Finally, we provide estimates of how such an event will develop under unabated global warming.

2. Material and Methods

2.1. Newspaper Articles About Heat-Related Impacts

We collected information from newspaper articles about heat-related impacts from the 2018 event. This does not include information about record-breaking temperatures, which were much more widespread. However, an exhaustive media overview was not the scope of this study.

2.2. Observation-Based Data

As an observational data basis, we use daily temperature from ERA-40 (40-year European Centre for Medium-Range Weather Forecasts Reanalysis; Uppala et al., 2005) for the period 1958–1999 and ERA-Interim (European Centre for Medium-Range Weather Forecasts Interim reanalysis; Dee et al., 2011) data for the period 1979–2018. We merged the ERA-40 and ERA-Interim data to cover a period from January 1958 to December 2018, with ERA-Interim starting in January 1979. We tested the consistency between ERA-40 and ERA-Interim by computing the root-mean-square error and mean bias between both data sets for the overlapping period (1979–1999). Both metrics show rather small difference between the data sets, in particular in the study region (see section 2.4 and supporting information Figure S1).

2.3. Climate Models

We use single runs from 29 climate models from the Coupled Model Intercomparison Project phase 5 (CMIP5) from the historical and future simulations (Taylor et al., 2012) under a high-emission scenario (Representative concentration pathway 8.5 [RCP8.5]) from 1870 to 2100 (van Vuuren et al., 2011). We analyze daily air temperature (*tas* in CMIP5) over land to estimate concurrent hot day areas and also used sea surface temperature (*tos* in CMIP5) for computing global mean temperature (see below). The complete list of models is provided in supporting information Table S1.

2.4. Study Region

We focus on latitudes north of 30° of the "human-affected and human-affecting" regions that either have a high population density (above 30 km^{-2}) or are important agricultural areas as defined in Seneviratne et al. (2018) with a total area of 23.7×10^6 km^2. This study region is referred to as NH AgPop area hereafter (Figure 1a).

2.5. Definition of Hot Days and Concurrent Hot Day Area

In this study we investigate the extensive spatially distributed heat impacts of the 2018 boreal summer as a single event. We compute the daily 90th temperature percentile using a 31-day moving window for the reference period 1958–1988, resulting in a 90th percentile climatology of the reference period for each model and the observed data. Each day between May and July that exceeds the temperature of the respective calendar day in the 90th percentile climatology is defined as a hot day. We then regrid results from each model

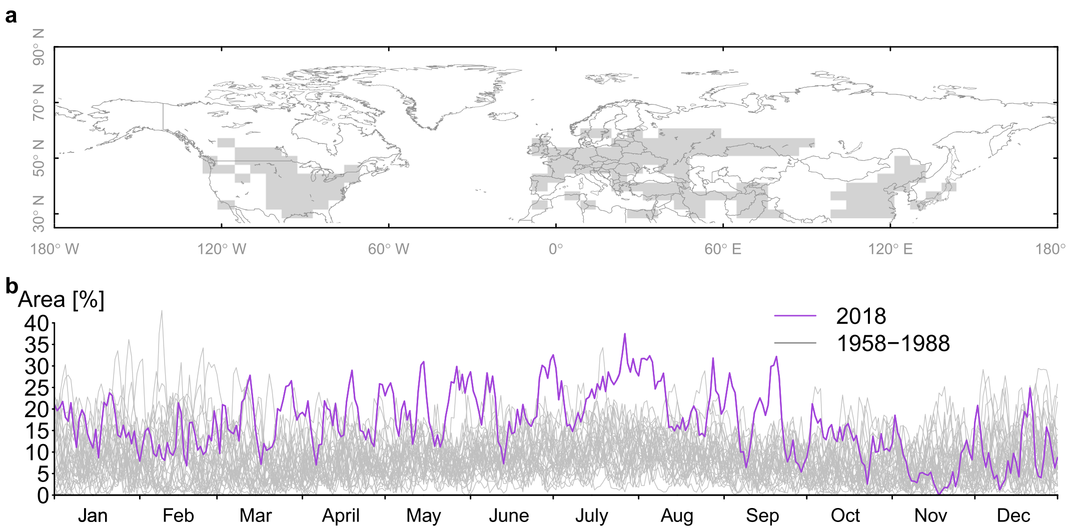

Figure 1. Considered hot day area and time frame. (a) Regions north of 30° latitude that either have a high population density (at least 30 people per square kilometer) or are agricultural regions (NH AgPop area) are highlighted in gray. (b) Annual time series of daily concurrent hot day area fraction of the NH AgPop area for 1959–1988 (gray) and 2018 (purple).

to the NH AgPop area grid and only consider the NH AgPop area for subsequent analyses. The average concurrent hot day area of a year is then defined as the average daily spatial extent of locations that experience a hot day between May and July. To obtain relative concurrent hot day areas, the average yearly concurrent hot day area is divided by the total area of the NH AgPop area. In addition to the concurrent hot day area between May and July, we also compute the concurrent hot day area between May to August and May to September (supporting information Figure S2).

2.6. The 2018 North Hemispheric Heat Extreme

The daily concurrent hot day area fraction over the target region is illustrated in Figure 1a. For the base period from 1958 to 1988 the daily area fraction that is concurrently affected by extreme warm or hot conditions covers on average 10% of the focus region (since we define hot day based on 90th percentile exceedances; see section 2.5). The 2018 area fraction exceeds the 1958 to 1988 areas by around a factor of 2 on average every day between May and July. The daily 2018 area peaks in the end of July reaching a maximum of 37.5% (Figure 1b). Hereafter, we focus on the temporal average between May and July 2018 as considered Global Concurrent Warm and Hot 2018 event, in short, GCWH18 extreme event.

2.7. Event Attribution

To estimate the human influence on climate extremes, a common approach is to compute the change in likelihood of events such as heat waves, droughts, and heavy precipitation events. Hereby, the ratio is calculated between the likelihood of the event in a climate with anthropogenic forcing (p_{CC}) and the likelihood in a reference period with smaller or no anthropogenic forcing (p_0; Fischer & Knutti, 2015; NAS, 2016; Stott et al., 2004, 2016). We quantify to what extent anthropogenic climate change has contributed to the probability of the GCWH18 event. To this end, we calculate the probability p_0 that the concurrent hot day area of 2018 would have occurred with little/without anthropogenic climate change. We further compute the probability p_{cc} that the concurrent hot day area of 2018 occurred with climate change. The ratio between the two probabilities $\frac{p_{cc}}{p_0}$, often referred to as risk ratio or probability ratio, allows statements about the human contribution to the event (NAS, 2016). If $p_0 = 0$, that is, the probability ratio equals ∞, the event could not have occurred without anthropogenic climate change. We compute p_0 for exceeding different concurrent hot day areas between 0% and 65% for the reference period (1958–1988) for CMIP5 models and observations. Since the climate has already warmed since preindustrial times by +0.28 °C, we perform the same computation for a preindustrial period (1870–1900). We further compute p_{cc} for different concurrent hot day areas for 31-year periods in which global warming reached +1 °C, +1.5 °C, and +2 °C for the same area thresholds (this results in slightly different 30-year periods for each model). For comparison, we also compute p_{cc} for the time period 1988–2018 (supporting information Figure S3).

10.1029/2019EF001189

a

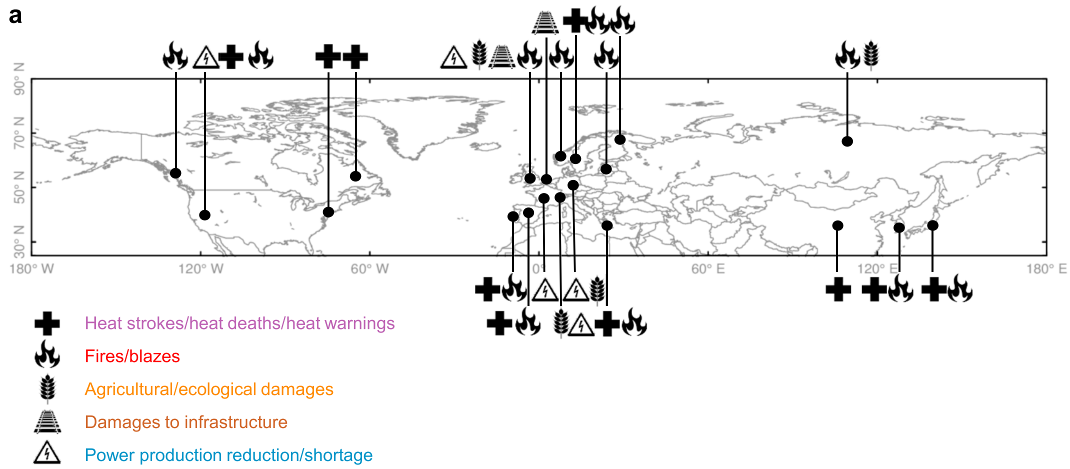

b

Country	Reported heat-related impact	Source
Canada	Quebec, 90 deaths in early July, more than 70 deaths	a, b
	British Columbia, wildfires, more than 12,984 km^2	c
China	heat warnings	d
Finland	Lapland, wildfires	e, f
France	closing of 4 nuclear power plants, reduction of nuclear power production	g, h
Germany	crop loss	c, h
	reduction of some power plants, reduction of power production from 3 coal-fired power plants	h, i
Greece	91 deaths (heat strokes, forest fires)	e
	80 deaths due to wildfires, more than 90 deaths due to wildfires	f, g
Japan	30 deaths, 119 deaths (heat strokes, forest fires), 77 heat deaths	b, e, j
	2,605 sent to hospitals in Tokyo, 30,000 people hospitalized	a, j
	heat warnings	j
Latvia	wildfires, 1,600 acres	f
Netherlands	melting of roads	g
Norway	wildfires	f
Portugal	heat/fire warnings	g
	forest fires, more than 1,000 hectares in Algarve	g
Russia	forest fires, wildfires in Siberia, Northern Russia 80,000 hectares	b, k, l
	crop loss	h
South Korea	29 death (heat strokes, forest fires)	e
Spain	3 deaths (heat strokes)	g
	fires	g
Sweden	49 fires, 62,000 acres, dozens of wildfires	a, f, g
	health warnings	f
Switzerland	high fish mortality in the Rhine	m
	crop loss	m
	reduction of nuclear power production in Muehleberg	n
United Kingdom	wildfires, blazes	b, o
	threat for garden birds, increase in the number of bloodsucking horseflies	o
	crop failure	b
	melting of roads, buckling of train tracks	o
	melting of the roof of a building	o
	reduction of power production of natural gas plants	h
United States	heat warnings for 35 million people	a
	California, 9 deaths (heat strokes, forest fires)	e
	New York City, at least 90,000 students who fail exams due to heat	b
	California, wildfires, 750,000 acres	k
	power shortage	o

Figure 2. Heat-related impacts in 2018 as reported by news agencies. (a) Approximate locations of heat-related impacts in the northern midlatitudes (above 30° north). The impacts are categorized according to heat impact (cross, purple text), fires (fire, red text), agricultural and ecological damages (wheat, orange text), damages to infrastructure (railway track, brown text), and impacts on power production reduction/shortage (warning signal, blue text). (b) Detailed heat-related impacts per country. The color refers to the categories in (a). The sources where this information is taken from are listed in Table 1.

Table 1
Overview of Media Articles for Heat-Related Impacts 2018

Reference	Press agency	Country	Article URL[a]	Published
a	New York Magazine	United States	http://nymag.com/daily/intelligencer/2018/07/a-global-heat-wave-has-set-the-arctic-circle-on-fire.html	20 July
b	Deutsche Welle	Germany	https://www.dw.com/en/the-global-heat-wave-thats-been-killing-us/a-44699601	18 July
c	Canadian Broadcasting Corporation (CBC)	Canada	https://www.cbc.ca/news/canada/british-columbia/state-emergency-bc-wildfires-1.4803546	30 August
d	XinhuaNet	China	http://www.xinhuanet.com/english/2018-07/31/c137359563.htm	31 July
e	The Guardian	United Kingdom	https://www.theguardian.com/environment/2018/aug/17/world-waking-up-to-reality-climate-change-hothouse-earth-author?CMP=sharebtntw	19 August
f	Los Angeles Times	United States	http://www.latimes.com/world/la-fg-wildfires-europe-20180728-story.html	28 July
g	British Broadcasting Corporation (BBC)	United Kingdom	https://www.bbc.com/news/world-europe-45070498	6 August
h	Bloomberg	United States	https://www.bloomberg.com/news/features/2018-07-25/heatwave-hits-commodities-from-crops-in-texas-to-french-power	25 July
i	Frankfurter Allgemeine Zeitung (FAZ)	Germany	http://www.faz.net/aktuell/wirtschaft/stromproduktion-gedrosselt-kraftwerke-wegen-hitze-vorabschaltung-15709562.html	26 July
j	Japan Times	Japan	https://www.japantimes.co.jp/news/2018/07/23/national/temperature-tokyo-hits-nationwide-high-year-mercury-rises-40-8-western-city-ome/#.W3pq5Jx9jOG	23 July
k	Washington Post	United States	https://www.washingtonpost.com/news/capital-weather-gang/wp/2018/08/17/red-hot-planet-this-summers-punishing-and-historic-heat-in-7-maps-and-charts/?noredirect=on&utmterm=.e878c76a8f3a	17 August
l	The Guardian	United Kingdom	https://www.theguardian.com/environment/2018/jul/13/heatwave-sees-record-high-temperatures-set-around-world-this-week	13 July
m	Tagesanzeier	Switzerland	https://www.tagesanzeiger.ch/wirtschaft/unternehmen-und-konjunktur/hitze-fuehrt-zu-erheblichen-ernteausfaellen/story/10299748	27 July
n	20 Minuten	Switzerland	https://www.20min.ch/schweiz/news/story/AKW-Muehleberg-drosselt-Leistung-wegen-Hitzewelle-11777563?httpredirect	27 July
o	The Guardian	United Kingdom	https://www.theguardian.com/uk-news/2018/jul/01/ten-top-facts-about-uk-summer-weather-heatwave	1 July

[a]Last access for all articles 7 May 2019.

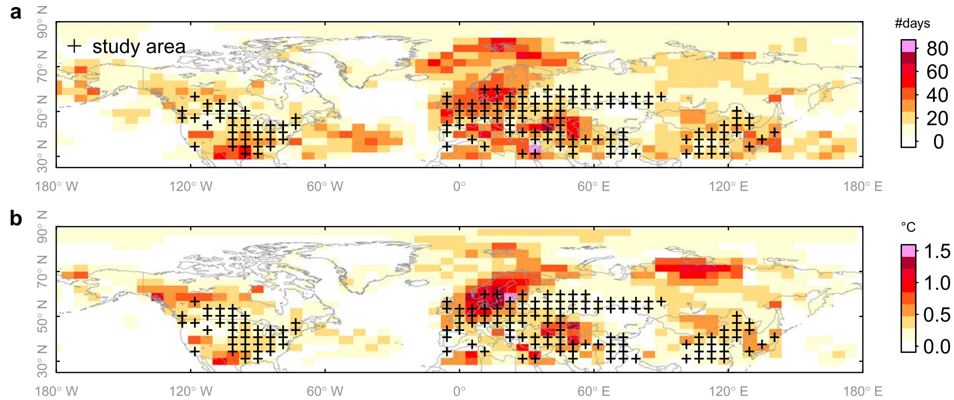

Figure 3. North hemispheric extent of the 2018 heat wave.(a) Number of hot days between May and July 2018. (b) Mean temperature anomalies of hot days between May and July compared to the 90th percentile climatology of daily temperatures in the reference period 1958–1988.

2.8. Global Mean Temperature

We estimate global mean temperature increase in CMIP5 models by computing 31-year moving averages of global mean temperature (T_{glob}) for all models between 1958 and 2100 and determine changes relative to the observational reference period 1958–1988. We estimate T_{glob} as weighted mean between *tas* over land and (dynamic) sea ice regions and sea surface temperature (*tos* in CMIP5) over the oceans, similar to observations (also called "blended temperatures" Cowtan et al., 2015). The multimodel mean warming between the reference period and 1870–1900 is +0.28 °C and is added to changes relative to the reference period. The warming levels of 1, 1.5, and 2 °C are determined as 31-year periods such that T_{glob} in the center year is closest to the respective warming level. For the scaling of T_{glob} with the concurrent hot day area, we relate the center year of each 31-year mean T_{glob} with the its respective concurrent hot day area. We use a distance weighting of each individual model to obtain values closest to T_{glob} and then compute multimodel median and interquartile range. We then apply a linear filter by 0.1 °C to smooth the data and improve the visual appearance.

3. Results

3.1. Concurrent 2018 Heat Impacts Across the Northern Hemisphere

Between May and July 2018, heat-related impacts have been described for at least 18 countries in the northern midlatitudes for different sectors, Figure 2 showcases a number of reported impacts. The URLs and news agencies of the media articles are provided in Table 1. Affected countries include Canada and the United States in North America, many European countries, as well as Russia, China, Japan, and South Korea in Asia. The wide spatial extent of impacts illustrates the global dimension of the extreme temperatures. News agencies reported direct heat-related impacts on humans and also on agriculture, power plants, and infrastructure (Figure 2b). For instance, in Quebec, more than 70 people died from heat strokes. In the United States, around 35 million people lived with regular heat warnings through July. In Japan, at least 30 people died and more than 2,500 were sent to hospital. Devastating fires destroyed vast amounts of intact forests in Canada, the United States, Norway, Sweden, Finland, Latvia, Greece, and South Korea. The hot temperatures also caused crop loss particularly for grains in Germany, Russia, Switzerland, and the United Kingdom. The heat wave conditions further led to power shortages and reduction in power production in the United States, Germany, France, and Switzerland. Roads melted and train tracks buckled in the Netherlands and the United Kingdom.

3.2. Extensive 2018 North Hemispheric Concurrent Hot Day Area

Between May and July 2018, some regions experienced hot days for up to 2 months, including Scandinavia, central Europe, and the United States (Figure 3a). The mean temperature anomaly of the hot days in these regions was up to 1.4 °C warmer than the 90th percentile daily temperatures in the reference period (Figure 3b). Owing to the associated exposure, heat wave impacts were particularly severe over the NH AgPop regions (see section 2.5).

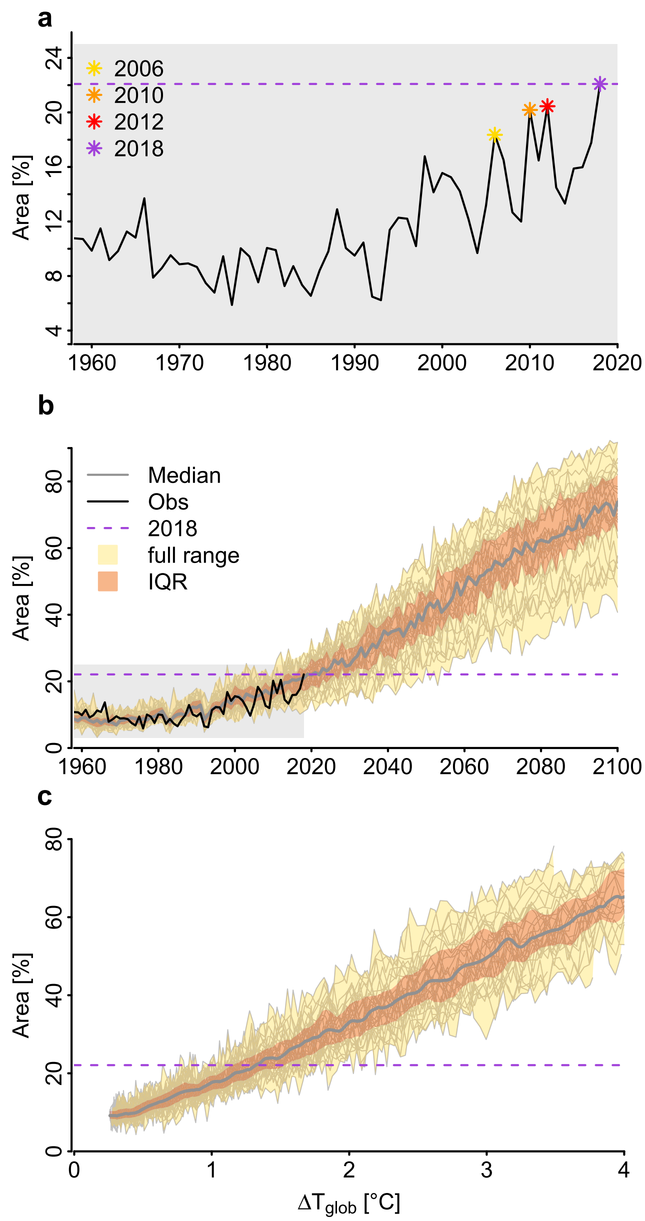

Figure 4. Temporal evolution of average concurrent hot day areas between May and July in observations and Earth system models. (a) Observed average concurrent hot day area between May and July in percent of the NH AgPop area for the time period 1958 to 2018. (b) Modeled average concurrent hot day area from 1958 to 2100 based on Coupled Model Intercomparison Project phase 5 models. The observed time series is shown in black; the range of (a) is highlighted in gray. (c) Modeled concurrent hot day area as a function of global mean temperature (T_{glob}) increase (see section 2.8). The 2018 event is highlighted by a horizontal purple line in each subpanel. For the models, we used a high-emission scenario (RCP8.5). We show the model median (gray), interquartile range (red), and the full model range (yellow).

Between May and July 2018, a daily average of about 22% of the NH AgPop area experienced a heat wave (Figure 4a). This extreme spatial extent of the GCWH18 event is unprecedented in the observational record when considering heat wave between May and July and nearly 8% larger then the second largest event of this kind in 2012. Computing the concurrent hot day area between May and August, 2010 and 2018 have a similar extent (23% and 22%; Figure S2a) and also for May to September (both 21%; Figure S2b).

For the high-emissions scenario (RCP8.5, section 2.3), the average concurrent hot day area during May and July is projected to cover more than 70% (multimodel median) of the NH AgPop area every day at the end of the 21st century (Figure 4b). The average concurrent hot day area scales approximately linearly with

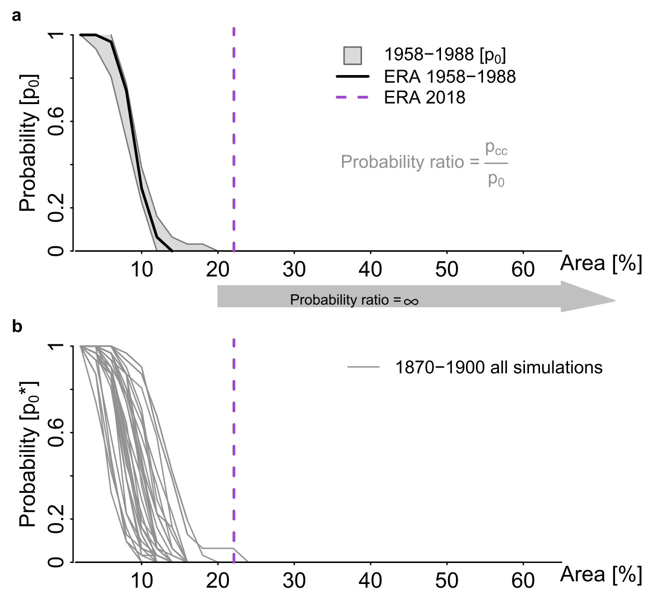

Figure 5. The 2018 north hemispheric concurrent heat extremes in an attribution framework. Shown are average north hemispheric concurrent hot day area thresholds (May to July) relative to the full NH AgPop area (0% to 65%) versus probabilities of exceeding that concurrent hot day area. The GCWH18 area is highlighted by a purple vertical dashed line in each subpanel. (a) Probabilities for exceeding concurrent hot day areas in the reference period 1958–1988 (p_0) for the multimodel ensemble (gray range) and observations (black line). The gray arrow indicates concurrent hot day area thresholds where $p_0 = 0$, and thus, the probability ratio $\frac{p_{cc}}{p_0}$ is infinity independent of p_{CC}. (b) Probabilities for exceeding concurrent hot day areas in the preindustrial period 1870–1900 (p_0^*). Each gray line represents one model simulation ($n = 29$). (c) Multimodel range of probabilities for exceeding concurrent hot day areas for global warming of +1 °C (orange), +1.5 °C (red), and +2 °C (dark red) with respect to 1870–1900. The boxplots indicate the distributions of the exceedance probabilities of the multimodel ensemble for the 2018-like concurrent hot day area (22%) for the different warming levels.

global mean temperature increases between +1 and +4 °C, with an increase of about 16% of the NH AgPop area per degree Celsius warming (Figure 4c). The warming in 2018 in the CMIP5 models since 1870–1900 is about +1.2 °C, which is slightly larger than current estimates based on observations (Intergovernmental Panel on Climate Change [IPCC] , 2018) and is related to data coverage, the choice of reference period, and interannual variability (see section 4).

3.3. Human Influence on the 2018 Concurrent Hot Day Area

The intense warming over the last decades has strongly shifted the odds of experiencing a GCWH18-like event, and we determine the human influence on a GCWH18-like area. A 2018-like event with an average 22% concurrent hot day area between May and July is not uncommon in climate simulations of a present-day climate with anthropogenic forcing ($p_{CC} > 0$). However, it does not occur in the model simulations of the reference period about 50 years earlier with much smaller anthropogenic forcing($p_0 = 0$). Thus, conditional on the analyzed climate models, the probability ratio of this event $\frac{p_{cc}}{p_0}$ is infinity. Hence, the analysis based on the 1958–1988 reference period suggests that average concurrent hot day areas that exceed 20% of the NH AgPop area could not have occurred without human-induced climate change. For the reference period, the observed probabilities of exceeding specific average concurrent hot day areas fall within the model range, which provides confidence in the model simulations of concurrent hot day areas with large extent (Figure 5a). However, this reference period is relatively short and already includes a mean warming signal of about 0.3 °C compared to the preindustrial period 1870 to 1900. During that period, the occurrence of a 2018-like heat event occurs in 2 years in one out of 29 models (Figure 5b). Hence, considering all model simulations, this results in an approximately 0.2% probability for a GCWH18-like area to have occurred under preindustrial conditions. These findings confirm that it is *virtually certain* (Mastrandrea et al., 2010) that the 2018 heat event would not have occurred without human-induced greenhouse gas emissions.

North hemispheric 2018-like or larger concurrent hot day areas are rare in today's climate (+1 °C mean warming; IPCC, 2018), with a likelihood of occurrence of 16% in the multimodel median (Figure 6a). Using

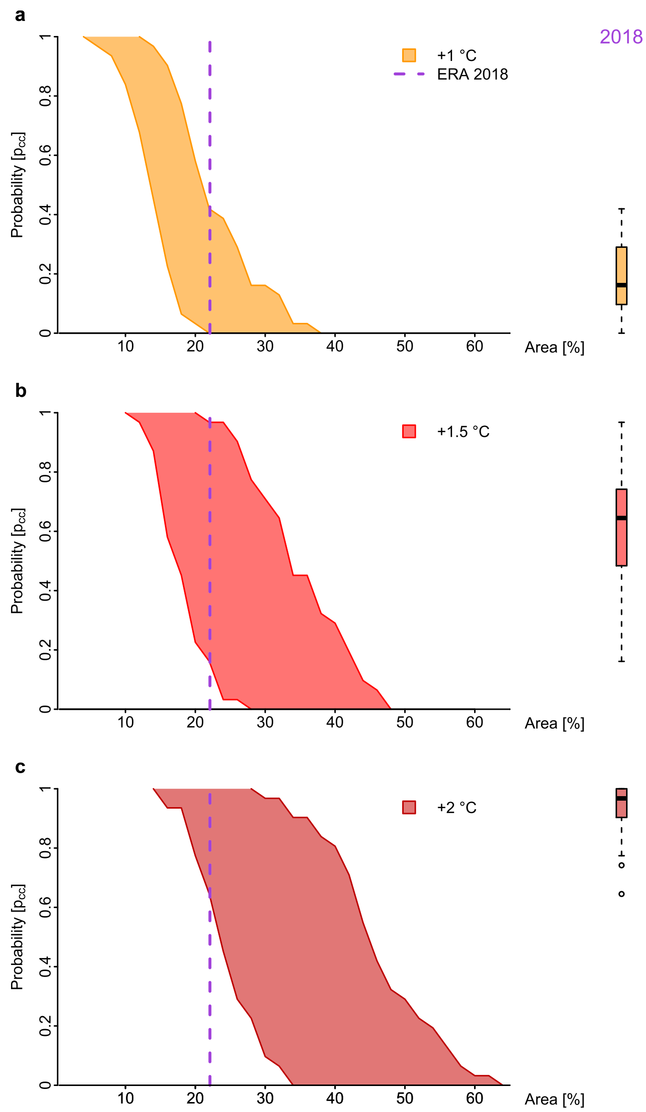

Figure 6. North hemispheric concurrent hot day area thresholds (May to July) relative to the full NH AgPop area (0% to 65%) versus multimodel range of probabilities of exceeding that concurrent hot day area for global warming of +1 °C (a), +1.5 °C (b), and +2 °C (c) with respect to 1870–1900. The GCWH18 area is highlighted by a purple vertical dashed line in each subpanel. The boxplots indicate the distributions of the exceedance probabilities of the multimodel ensemble for the 2018-like concurrent hot day area (22%) for the different warming levels.

a present-day period from 1988 to 2018 (with RCP8.5 forcing after 2005), the multimodel median probability of a GCWH18-like event is reduced to 6% (supporting information Figure S3).

In a +1.5 and +2 °C world, the probability of experiencing a heat wave with at least the size of the GCWH18 event increases to 65% (Figure 6b) and 97% (Figure 6c) in the multimodel median, respectively. This implies that even if global warming is limited to +1.5 °C, we would experience a GCWH18-type event on average nearly 2 out of 3 years and nearly every year at +2 °C warming.

4. Discussion and Conclusions

Over the recent decades, we have seen a strong increase in land areas that are concurrently affected by warm and hot temperatures (Figure 4a). The four largest events in the observational record occurred within the last 12 years, consistent with a strong recent increase in heat wave occurrence (Christidis et al., 2014; Rowe & Derry, 2012; Seneviratne et al., 2014). Generally, the large interannual variability of concurrent heat wave occurrence can be driven by different processes. While years with El Niño events are typically associated with warmer temperatures at a global scale (Seneviratne et al., 2014), this effect is less relevant for the boreal summers in the NH AgPop region. Furthermore, changes in large-scale circulation and land-atmosphere feedbacks could increase the areas concurrently experience warm and hot temperatures. A recent study shows that in 2018 a specific atmospheric pattern connected heat waves in North America, Western Europe, and the Caspian Sea region (Kornhuber et al., 2019). Additionally, central Europe experienced concurrent dry and hot conditions from spring to summer in 2018 that were exceptional at least within the last 500 years (Toreti et al., 2019). The dry conditions in central and Northern Europe possibly amplified extreme temperatures in these regions via land-atmosphere feedbacks.

Overall, our results suggest that we have entered a new climate regime in which the occurrence of extraordinary global-scale heat waves cannot be explained without human-induced climate change. In particular, the simulations show that a GCWH18-like event does not occur in historical simulations. The saturation effect of the probability ratio will become more dominant in a warmer climate where unprecedented events will have a probability ratio in the mathematical limit of $\frac{p_{cc}}{p_0} = \infty$ (Harrington & Otto, 2018).

The importance of global warming targets for limiting the occurrence of global-scale heat waves becomes even more apparent when considering climate model projections. We find that the probability of devastating 2018-like areas to occur will increase drastically (from 65% to 97%) if global mean temperatures shift from +1.5 °C to +2 °C. This is consistent with the recently approved IPCC special report on Global Warming of 1.5 °C, which finds significantly stronger climate-related impacts for +2 °C compared to +1.5 °C warming (IPCC, 2018).

However, determining impacts conditioned on global mean temperature targets is not free of uncertainties. Using only 2-m air temperature (*tas* in CMIP5) for computing T_{glob} leads to an overestimation of the CMIP5 multimodel median of global mean temperature of 0.18 °C compared to observed temperatures for the time period 2000–2009 with respect to 1861–1880 (Richardson et al., 2016). This offset is partly related to a reduced coverage in the observations (Cowtan et al., 2015). For instance, Antarctica is not well covered by observations and warms faster than the global average (Cowtan & Way, 2014). It is not clear how the coverage will change in future; hence, here we consider the whole globe instead of assuming future changes in coverage. In addition to the effects of data coverage, observation-based estimates of global mean temperature use air temperature over land and sea ice but sea surface temperatures over oceans (Cowtan et al., 2015; Medhaug et al., 2017; Richardson et al., 2016). To account for this, we compute T_{glob} as "blended temperatures" (Cowtan et al., 2015), that is, using air temperature over land and (dynamic) sea ice regions and sea surface temperature over the oceans (see section 2.8). This leads to a present-day warming of +1.22 °C compared to +1.29 °C when only *tas* is considered (supporting information Figure S3). Further differences between models and observations can be related to internal climate variability, overestimated radiative forcing in models, and model response error (Flato et al., 2013). Observations themselves are also uncertain with differences in mean global warming in the early 2000s of up to +0.4 °C (Medhaug et al., 2017). Finally, the global mean temperature change also depends on the preindustrial reference period, which can lead to a shift of a decade to reach a specific warming level (Hawkins & Sutton, 2016). Overall, because of these systematic differences between CMIP5 models and observations, our estimates of future exceedance probabilities at specific global mean temperature targets are conservative estimates.

Our results demonstrate that the GCWH18 extreme event could not have occurred without human-induced climate change. Due to taking averages over large areas, the signal-to-noise ratio is high for such events, and we could exclude that it could have occurred as part of natural variability. To our knowledge, so far only for marine heat waves, it could be concluded that their occurrence would not have been possible without climate change (Oliver et al., 2018; Perkins-Kirkpatrick et al., 2019). Thus, the GCWH18 event possibly constitutes the first climate phenomenon on land that has been uniquely attributed to human-induced global warming.

Heat waves will likely reach highly dangerous levels for ecosystems and societies over the coming decades. However, if other factors that contribute to such impacts change as well, assessing environmental risks associated with heat waves becomes much more complex. For instance, the impact of expanding concurrent hot day areas is often aggravated by population increases. In the United States, population exposure to extreme heat has increased fourfold to sixfold in the late twentieth century due to a combined increase in temperatures and population growth (Jones et al., 2015).

In contrast to the local heat impacts on population, widely spread agricultural regions can serve as an integrator of heat-related impacts on crop yields (Lobell & Field, 2007). Concurrent heat extremes in different agricultural regions can amplify heat impacts as simultaneous production shocks can increase global food prizes and food insecurity (Tigchelaar et al., 2018). Multiple heat waves that occur subsequently in the same region can amplify heat wave impacts and are projected to increase with global warming (Baldwin et al., 2019). Furthermore, a higher probability of experiencing a heat wave naturally increases the likelihood of compound extremes. In particular, the co-occurrence rate of compound drought-heat wave events will increase even if there is no trend in drought occurrence (Diffenbaugh et al., 2015; Zscheischler & Seneviratne, 2017) and may exacerbate heat-related impacts (Miralles et al., 2018; Seneviratne et al., 2010). Such compound events in space and time are challenging to analyze but require immediate attention because climate change will shift many aspects of these events (Zscheischler et al., 2018).

The provided scaling relationship for concurrent hot day areas (Figure 4c) can help to assess future risk of heat-related impacts. However, it also illustrates that concomitant heat waves in large parts of the inhabited and agricultural land area in the northern midlatitudes can be effectively prevented by limiting global warming. To avoid major future impacts associated with human-induced global heat waves, we have to take ambitious mitigation actions to strongly reduce greenhouse gas emissions.

Acknowledgments
M. M. V., S. I. S., and R. W. acknowledge funding from the European Research Council (ERC) "DROUGHT-HEAT" project under Grant agreement FP7–IDEAS ERC–617518. J. Z. acknowledges financial support from the Swiss National Science Foundation (Ambizione Grant 179876). The ERA-40 reanalysis data are available online (https://apps.ecmwf.int/datasets/data/era40-daily/). The ERA-Interim reanalysis data sets are available online (http://www.ecmwf.int/en/research/climate-reanalysis/era-interim). The CMIP5 model simulations are available from respecting modeling listed in supporting information Table S1.

References

Baldwin, J. W., Dessy, J. B., Vecchi, G. A., & Oppenheimer, M. (2019). Temporally compound heat wave events and global warming: An emerging hazard. *Earth's Future*, *7*, 411–427. https://doi.org/10.1029/2018EF000989

Barriopedro, D., Fischer, E. M., Luterbacher, J., Trigo, R. M., & García-Herrera, R. (2011). The hot summer of 2010: Redrawing the temperature record map of Europe. *Science*, *332*(6026), 220–224.

Berghuijs, W. R., Allen, S. T., Harrigan, S., & Kirchner, J. W. (2019). Growing spatial scales of synchronous river flooding in europe. *Geophysical Research Letters*, *46*, 1423–1428. https://doi.org/10.1029/2018GL081883

Christidis, N., Jones, G., & Stott, P. A. (2014). Dramatically increasing chance of extremely hot summers since the 2003 European heatwave. *Nature Climate Change*, *5*, 46–50.

Copernicus (2019). European state of the climate 2018. Summary. Copernicus Climate Change Service, European Centre for Medium-Range Weather Forecasts, https://climate.copernicus.eu/sites/default/files/2019-04/Brochure_Final_Interactive.pdf

Coumou, D., & Rahmstorf, S. (2012). A decade of weather extremes. *Nature Climate Change*, *2*, 491–496.

Coumou, D., & Robinson, A. (2013). Historic and future increase in the global land area affected by monthly heat extremes. *Environmental Research Letters*, *8*(3), 34018.

Cowtan, K., Hausfather, Z., Hawkins, E., Jacobs, P., Mann, M. E., Miller, S. K., et al. (2015). Robust comparison of climate models with observations using blended land air and ocean sea surface temperatures. *Geophysical Research Letters*, *42*, 6526–6534. https://doi.org/10.1002/2015GL064888

Cowtan, K., & Way, R. G. (2014). Coverage bias in the HadCRUT4 temperature series and its impact on recent temperature trends. *Quarterly Journal of the Royal Meteorological Society*, *140*(683), 1935–1944.

Dee, D. P., Uppala, S. M., Simmons, a. J., Berrisford, P., Poli, P., Kobayashi, S., et al. (2011). The ERA-Interim reanalysis: Configuration and performance of the data assimilation system. *Quarterly Journal of the Royal Meteorological Society*, *137*(656), 553–597.

Diffenbaugh, N. S., Swain, D. L., & Touma, D. (2015). Anthropogenic warming has increased drought risk in California. *Proceedings of the National Academy of Sciences*, *112*(13), 3931–3936.

Fischer, E. M., & Knutti, R. (2015). Anthropogenic contribution to global occurrence of heavy-precipitation and high-temperature extremes. *Nature Climate Change*, *5*, 560–564.

Flato, G., Marotzke, J., Abiodun, B., Braconnot, P., Chou, S. C., Collins, W., et al. (2013). Evaluation of climate models. In T. F. Stocker, D Qin, G.-K. Plattner, M. Tignor, S. K. Allen, J. Boschung, et al. (Eds.), *Climate change 2007: The physical science basis. Contribution of working group I to the fourth assessment report of the intergovernmental panel on climate change* (pp. 741–866). Cambridge, United Kingdom and New York, NY, USA: Cambridge University Press.

Frölicher, T. L., Fischer, E. M., & Gruber, N. (2018). Marine heatwaves under global warming. *Nature*, *560*(7718), 360–364.

Harrington, L. J., & Otto, F. E. L. (2018). Adapting attribution science to the climate extremes of tomorrow. *Environmental Research Letters*, *13*(12), 123006.

Hawkins, E., & Sutton, R. (2016). Connecting climate model projections of global temperature change with the real world. *Bulletin of the American Meteorological Society*, *97*(6), 963–980.

IPCC (2018). Summary for policymakers. In V. Masson-Delmotte, P. Zhai, H. O. Pörtner, D. Roberts, J. Skea, P. R. Shukla, et al. (Eds.), *Global warming of 1.5 °c. An IPCC special report on the impacts of global warming of 1.5 °c above pre-industrial levels and related global greenhouse gas emission pathways, in the context of strengthening the global response to the threat of climate change, sustainable development, and efforts to eradicate poverty* (pp. 32). Geneva, Switzerland: World Meteorological Organization.

Jones, B., O'Neill, B. C., McDaniel, L., McGinnis, S., Mearns, L. O., & Tebaldi, C. (2015). Future population exposure to US heat extremes. *Nature Climate Change*, *5*, 652–655.

Kornhuber, K., Osprey, S., Coumou, D., Petri, S., Petoukhov, V., Rahmstorf, S., & Gray, L. (2019). Extreme weather events in early summer 2018 connected by a recurrent hemispheric wave-7 pattern. *Environmental Research Letters*, *14*(5), 054002. https://doi.org/10.10882F1748-93262Fab13bf

Lobell, D. B., & Field, C. B. (2007). Global scale climate-crop yield relationships and the impacts of recent warming. *Environmental Research Letters*, *2*(1), 14002.

Mastrandrea, M., Field, C., Stocker, T., Edenhofer, O., Ebi, K., Frame, D., et al. (2010). Guidance note for lead authors of the IPCC fifth assessment report on consistent treatment of uncertainties. Intergovernmental Panel on Climate Change (IPCC).

Medhaug, I., Stolpe, M. B., Fischer, E. M., & Knutti, R. (2017). Reconciling controversies about the global warming hiatus. *Nature*, *545*, 41–47.

Miralles, D. G., Gentine, P., Seneviratne, S. I., & Teuling, A. J. (2018). Land–atmospheric feedbacks during droughts and heatwaves: State of the science and current challenges. *Annals of the New York Academy of Sciences*, *1436*, 19–35.

NAS (2016). *Attribution of extreme weather events in the context of climate change*. Washington, DC, USA: The National Academies Press.

NOAA (2018a). Global climate report for July 2018. National Centers for Environmental Information, https://www.ncdc.noaa.gov/sotc/global/201807

NOAA (2018b). Global climate report for June 2018. National Centers for Environmental Information, https://www.ncdc.noaa.gov/sotc/global/201806

NOAA (2018c). Global climate report for May 2018. National Centers for Environmental Information, https://www.ncdc.noaa.gov/sotc/global/201805

Oliver, E. C. J., Perkins-Kirkpatrick, S. E., Holbrook, N. J., & Bindoff, N. L. (2018). Anthropogenic and natural influences on record 2016 marine heat waves. *Bulletin of the American Meteorological Society*, *99*(1), S44–S48.

Otto, F. E. L., Massey, N., van Oldenborgh, G. J., Jones, R. G., & Allen, M. R. (2012). Reconciling two approaches to attribution of the 2010 Russian heat wave. *Geophysical Research Letters*, *39*, L04702. https://doi.org/10.1029/2011GL050422

Perkins-Kirkpatrick, S. E., King, A. D., Cougnon, E. A., Holbrook, N. J., Grose, M. R., Oliver, E. C. J., et al. (2019). The role of natural variability and anthropogenic climate change in the 2017/18 Tasman sea marine heatwave. *Bulletin of the American Meteorological Society*, *100*(1), S105–S110.

Rahmstorf, S., & Coumou, D. (2011). Increase of extreme events in a warming world. *Proceedings of the National Academy of Sciences*, *108*(44), 17,905–17,909.

Ratnam, J. V., Behera, S. K., Ratna, S. B., Rajeevan, M., & Yamagata, T. (2016). Anatomy of Indian heatwaves. *Scientific Reports*, *6*, 24395.

Richardson, M., Cowtan, K., Hawkins, E., & Stolpe, M. B. (2016). Reconciled climate response estimates from climate models and the energy budget of Earth. *Nature Climate Change*, *6*, 931–935.

Rowe, C. M., & Derry, L. E. (2012). Trends in record-breaking temperatures for the conterminous United States. *Geophysical Research Letters*, *39*, L16703. https://doi.org/10.1029/2012GL052775

Sarhadi, A., Ausín, M. C., Wiper, M. P., Touma, D., & Diffenbaugh, N. S. (2018). Multidimensional risk in a nonstationary climate: Joint probability of increasingly severe warm and dry conditions. *Science Advances*, *4*(11), eaau3487.

Seneviratne, S. I., Corti, T., Davin, E. L., Hirschi, M., Jaeger, E. B., Lehner, I., et al. (2010). Investigating soil moisture-climate interactions in a changing climate: A review. *Earth-Science Reviews*, *99*(3-4), 125–161.

Seneviratne, S. I., Donat, M. G., Mueller, B., & Alexander, L. V. (2014). No pause in the increase of hot temperature extremes. *Nature Climate Change*, *4*, 161–163.

Seneviratne, S. I., Phipps, S. J., Pitman, A. J., Hirsch, A. L., Davin, E. L., Donat, M. G., et al. (2018). Land radiative management as contributor to regional-scale climate adaptation and mitigation. *Nature Geoscience*, *11*(2), 88–96.

Stott, P. A., Christidis, N., Otto, F. E. L., Sun, Y., Vanderlinden, J.-P., van Oldenborgh, G. J., et al. (2016). Attribution of extreme weather and climate-related events. *Wiley Interdisciplinary Reviews: Climate Change*, *7*(1), 23–41.

Stott, P. A., Stone, D. A., & Allen, M. R. (2004). Human contribution to the European heatwave of 2003. *Nature*, *432*, 610–614.

Taylor, K. E., Stouffer, R. J., & Meehl, G. a. (2012). An overview of CMIP5 and the experiment design. *Bulletin of the American Meteorological Society*, *93*(4), 485–498.

Tigchelaar, M., Battisti, D. S., Naylor, R. L., & Ray, D. K. (2018). Future warming increases probability of globally synchronized maize production shocks. *Proceedings of the National Academy of Sciences*, *115*, 6644–6649.

Toreti, A., Belward, A., Perez-Dominguez, I., Naumann, G., Manfron, G., Jürg, L., et al. (2019). The exceptional 2018 European water seesaw calls for action on adaptation. *Earth's Future*. https://doi.org/10.1029/2019EF001170

Uppala, S. M., KÅllberg, P. W., Simmons, A. J., Andrae, U., Da Costa Bechtold, V., Fiorino, M., et al. (2005). The ERA-40 re-analysis. *Quarterly Journal of the Royal Meteorological Society*, *131*(612), 2961–3012.

van Vuuren, D. P., Edmonds, J., Kainuma, M., Riahi, K., Thomson, A., Hibbard, K., et al. (2011). The representative concentration pathways: An overview. *Climatic Change*, *109*(1), 5–31.

Wehner, M., Stone, D., Krishnan, H., AchutaRao, K., & Castillo, F. (2016). The deadly combination of heat and humidity in India and Pakistan in summer 2015. *Bulletin of the American Meteorological Society*, *97*(12), 81–86.

World Weather Attribution (2018). Heatwave in Northern Europe, Summer 2018. last access 5 Oct 2018.

Zscheischler, J., & Seneviratne, S. I. (2017). Dependence of drivers affects risks associated with compound events. *Science Advances*, *3*(6), e1700263.

Zscheischler, J., Westra, S., van den M., H. B. J. J., Seneviratne, S. I., Ward, P. J., Pitman, A., et al. (2018). Future climate risk from compound events. *Nature Climate Change*, *8*(6), 469–477.